Supplement of Atmos. Chem. Phys., 23, 3861–3885, 2023
https://doi.org/10.5194/acp-23-3861-2023-supplement

Atmospheric Chemistry and Physics
Open Access

Supplement of

Insights into the single-particle composition, size, mixing state, and aspect ratio of freshly emitted mineral dust from field measurements in the Moroccan Sahara using electron microscopy

Agnesh Panta et al.

Correspondence to: Agnesh Panta (agnesh@geo.tu-darmstadt.de)

1 SEM classification scheme

In this study, a scanning electron microscope (FEI ESEM Quanta 400 FEG instrument, Eindhoven, The Netherlands) equipped with an X-Max 150 Energy-Dispersive X-ray spectroscopy (EDX) silicon drift X-ray detector (Oxford, Oxfordshire, UK) was used for obtaining the elemental composition of individual particle. The table below is a description of the classification scheme and the observed particle groups. Note that the given method cannot be used to quantify the percentage of C, N, and O due to their high uncertainty and substrate contributions. Particle classes are named for their most prevalent component(s), which may contain terms for mineral phases to simplify the naming (e.g. gypsum, quartz). Those mineral phases were chosen as the most prevalent components that matched the reported elemental composition, but no real phase identification of individual particles (e.g., by transmission electron microscopy) was carried out. Therefore, all the particle classes are termed '-like' to express the similarity in chemical fingerprints.

Table S1: Definition of particle classes derived from elemental composition.

Particle class	Criteria
Hematite-like	Fe/(Na+Mg+Al+Si+P+S+Cl+K+Ca+Ti+Cr+Mn+Fe)=0.5 .. 0.98999 & Cr/(Cr+Fe)=0 .. 0.1 & Cl/(Cl+Fe)=0 .. 0.1 & (F+Si)/(F+Na+Mg+Al+Si+P+S+Cl+K+Ca+Ti+Cr+Mn+Fe)=0 .. 0.499 & Ti/Fe=0 .. 0.24999
Rutile-like	Ti/(Na+Mg+Al+Si+P+S+Cl+K+Ca+Ti+Cr+Mn+Fe)=0.7 .. 1.01 & Ca/(Ca+Ti)=0 .. 0.3
Ilmenite-like	(Fe+Ti)/(Na+Mg+Al+Si+P+S+Cl+K+Ca+Ti+Cr+Mn+Fe)=0.7 .. 1.01 & Ti/Fe=0.25 .. 4
Quartz-like	Si/(Na+Mg+Al+Si+P+S+Cl+K+Ca+Ti+Cr+Mn+Fe)=0.7 .. 1.01 & (Na+Mg+K+Ca+Al)/Si=0 .. 0.2 & F/(F+Si)=0 .. 0.499
Complex quartz-like	(Al+Si+Na+Mg+K+Ca+Fe) / (Na+Mg+Al+Si+P+S+Cl+K+Ca+Ti+Cr+Mn+Fe)=0.7 .. 1.01 & Al/Si=0.05 .. 0.25 & (Na+K+Ca)/Si=0 .. 1 & Fe/Si=0 .. 0.5 & Ca/Si=0 .. 0.5 & K/Si=0 .. 0.5 & Mg/Si=0 .. 0.5 & Na/Si=0 .. 0.5 & (Na+Cl+2*S) / (Al+Si)=0 .. 0.25
Microcline-like	(K+Al+Si) / (Na+Mg+Al+Si+P+S+Cl+K+Ca+Ti+Cr+Mn+Fe)=0.7 .. 1.01 & Al/Si=0.2 .. 0.45 & K/Si=0.15 .. 0.5 & Ca/Si=0 .. 0.1 & Na/Si=0 .. 0.1 & (Cl+2*S)/Na = 0 .. 0.3 & (Cl+2*S) / (Al+Si)=0 .. 0.125
Albite-like	(Na+Al+Si) / (Na+Mg+Al+Si+P+S+Cl+K+Ca+Ti+Cr+Mn+Fe)=0.7 .. 1.01 & Al/Si=0.2 .. 0.45 & Na/Si=0.15 .. 0.5 & Ca/Si=0 .. 0.1 & K/Si=0 .. 0.1 & (Cl+2*S)/Na = 0 .. 0.3 & (Cl+2*S) / (Al+Si)=0 .. 0.125
Complex feldspar-like	(Al+Si+Na+Mg+K+Ca+Fe) / (Na+Mg+Al+Si+P+S+Cl+K+Ca+Ti+Cr+Mn+Fe)=0.7 .. 1.01 & Al/Si=0.25 .. 0.5 & (Na+K+Ca)/Si=0.125 .. 0.7 & Fe/Si=0 .. 0.5 & Ca/Si=0 .. 0.5 & K/Si=0 .. 0.5 & Mg/Si=0 .. 0.5 & Na/Si=0 .. 0.5 & (Na+Cl+2*S) / (Al+Si)=0 .. 0.25
Complex clay/feldspar mixture	(Al+Si+Na+Mg+K+Ca+Fe) / (Na+Mg+Al+Si+P+S+Cl+K+Ca+Ti+Cr+Mn+Fe)=0.7 .. 1.01 & Al/Si=0.25 .. 0.5 & (Na+K+Ca)/Si=0 .. 0.125 & Fe/Si=0 .. 0.5 & Ca/Si=0 .. 0.5 & K/Si=0 .. 0.5 & Mg/Si=0 .. 0.5 & Na/Si=0 .. 0.5 & (Na+Cl+2*S) / (Al+Si)=0 .. 0.25
Mika-like	(Ca+Na+K+Fe+Mg+Al+Si) / (Na+Mg+Al+Si+P+S+Cl+K+Ca+Ti+Cr+Mn+Fe)=0.7 .. 1.01 & Al/Si=0.2 .. 3 & (Na+K+Ca+Mg+Fe)/(Si)=0.5 .. 2.5 & (Cl+2*S)/Na = 0 .. 0.3 & (Cl+2*S) / (Al+Si)=0 .. 0.125

Complex clay-mineral-like	(Al+Si+Na+Mg+K+Ca+Fe) / (Na+Mg+Al+Si+P+S+Cl+K+Ca+Ti+Cr+Mn+Fe)=0.7 .. 1.01 & Al/Si=0.5 .. 1.5 & (Mg+Fe+K)/Si=0.1 .. 1 & Fe/Si=0 .. 0.5 & Ca/Si=0 .. 0.5 & K/Si=0 .. 0.5 & Mg/Si=0 .. 0.5 & Na/Si=0 .. 0.5 & (Na+Cl+2*S) / (Al+Si)=0 .. 0.25
Illite-like	(K+Al+Si) / (Na+Mg+Al+Si+P+S+Cl+K+Ca+Ti+Cr+Mn+Fe)=0.7 .. 1.01 & Al/Si=0.45 .. 1.5 & Mg/(Al+Si)=0 .. 0.2 & Fe/(Al+Si)=0 .. 0.2 & (Na+Ca)/(Al+Si)=0 .. 0.2 & K/(Si)=0.1 .. 1.01 & (Na+Cl+2*S) / (Al+Si)=0 .. 0.25
Chlorite-like	(Mg+Fe+Al+Si) / (Na+Mg+Al+Si+P+S+Cl+K+Ca+Ti+Cr+Mn+Fe)=0.7 .. 1.01 & Al/Si=0.5 .. 1.5 & Fe/(Al+Si)=0.2 .. 1.01 & Ca/(Al+Si)=0 .. 0.3 & (Na+Cl+2*S) / (Al+Si)=0 .. 0.25
Smectite-like	(Mg+Al+Si) / (Na+Mg+Al+Si+P+S+Cl+K+Ca+Ti+Cr+Mn+Fe)=0.7 .. 1.01 & Al/Si=0.5 .. 1.5 & Fe/(Al+Si)=0 .. 0.2 & Mg/(Al+Si)=0.2 .. 1.01 & Ca/(Al+Si)=0 .. 0.2 & Na/(Al+Si)=0 .. 0.2 & K/(Si)=0 .. 0.1 & (Na+Cl+2*S) / (Al+Si)=0 .. 0.25
Kaolinite-like	(Al+Si)/(Na+Mg+Al+Si+P+S+Cl+K+Ca+Ti+Cr+Mn+Fe)=0.7..1.01 & Al/Si=0.5..1.5 & Fe/(Al+Si)=0..0.2 & Mg/(Al+Si)=0..0.2 & Ca/(Al+Si)=0..0.2 & Na/(Al+Si)=0..0.15 & K/(Si)=0..0.1 & (Na+Cl+2*S)/(Al+Si)=0..0.25
Ca-rich silicate/Ca-Si-mixture	(Ca+Al+Si) / (Na+Mg+Al+Si+P+S+Cl+K+Ca+Ti+Cr+Mn+Fe)=0.7 .. 1.01 & Ca/(Al+Si)=0.3 .. 3.333 & (Na+Cl+2*S) / (Al+Si)=0 .. 0.25
Calcite-like	Ca/(Na+Mg+Al+Si+P+S+Cl+K+Ca+Ti+Cr+Mn+Fe)=0.7 .. 1.01 & (Al+Si)/Ca=0 .. 0.3 & Mg/Ca=0 .. 0.3 & S/Ca=0 .. 0.3 & Cl/Ca=0 .. 0.3 & P/(Ca+P)=0 .. 0.19 & S/(Ca+S)=0 .. 0.19
Dolomite-like	(Mg+Ca) / (Na+Mg+Al+Si+P+S+Cl+K+Ca+Ti+Cr+Mn+Fe)=0.7 .. 1.01 & Mg/Ca=0.3 .. 3 & S/Ca=0 .. 0.3 & Cl/Ca=0 .. 0.3 & (Al+Si)/Ca=0 .. 0.3
Apatite-like	(Ca+P) / (Na+Mg+Al+Si+P+S+Cl+K+Ca+Ti+Cr+Mn+Fe)=0.7 .. 1.01 & Mg/Ca=0 .. 0.3 & P/(Ca+P)=0.2 .. 0.8 & Cl/Ca=0 .. 0.3 & (Al+Si)/(P+Ca)=0 .. 0.25
Gypsum-like	(Ca+S) / (Na+Mg+Al+Si+P+S+Cl+K+Ca+Ti+Cr+Mn+Fe)=0.7 .. 1.01 & Ca/(Ca+S)=0.2 .. 0.8 & Mg/Ca=0 .. 0.3 & Cl/Ca=0 .. 0.3
Alunite-like	(Al+K+S) / (Na+Mg+Al+Si+P+S+Cl+K+Ca+Ti+Cr+Mn+Fe)=0.7 .. 1.01 & Ca/(Ca+Al+K+S)=0 .. 0.05 & Si/(Si+Al+K+S)=0 .. 0.1 & K/(Al+K+S)=0.05 .. 0.3 & S/(Al+K+S)=0.15 .. 0.5 & Al/(Al+K+S)=0.3 .. 0.8

Halite-like	(Na+Mg+Cl) / (Na+Mg+Al+Si+P+S+Cl+K+Ca+Ti+Cr+Mn+Fe)=0.7 .. 1.01 & Cl/(Na+0.5*Mg)=0.5 .. 2 & Cl / (Cl+S)=0.7 .. 1.01 & S/(Na+0.5*Mg)=0 .. 0.2 & K/Na=0 .. 0.5 & Ca/Na=0 .. 0.5 & Mg/Na=0 .. 0.5 & (Al+Si) / (Na+Cl+S)=0 .. 0.25
Complex sulfate	(Na+Mg+K+Ca+S+Cl) / (Na+Mg+Al+Si+P+S+Cl+K+Ca+Ti+Cr+Mn+Fe)=0.7 .. 1.01 & (Al+Si)/S=0 .. 0.25 & Cl / (Cl+S)=0 .. 0.3 & IsNotInOtherGroup=yes & SSRIB=(Na+2*Mg+K+2*Ca-Cl-2*S)/(Na+2*Mg+K+2*Ca+Cl+2*S)

2 Particle types

Typical chemical compositions of a set of minerals and boundary rules were used to define particle groups (see S1 above). Based on the applied scheme, particles were assigned to the following classes: (i) oxides/hydroxides, (ii) feldspar, (iii) clay minerals, (iv) quartz-like and complex quartz-like, (v) other silicates (vi) Ca-rich, (vii) sulfates, and (viii) mixtures and others. However, it is important to note that each particle can be composed of different minerals and can have variable and even indistinguishable compositions. Therefore, the created groups may not only consist of the minerals described below.

2.1 Oxides/Hydroxides

This class consists of hematite-like and anatase-like particles with Fe and Ti X-ray signals dominating, respectively. Both particle types were found mainly in particles with $d_v < 2.5$ µm with anatase-like particles being rare. Iron (Fe) oxides are present both in pure crystalline form and as small impurities attached to other minerals. Moreover, Fe is present in other particle groups as well, mainly in clays and silicates. However, the presence of Fe can be due to not only Fe oxi(hydroxi)des but also to structural Fe. Fe oxides tend to exist as separate individual particles in sizes $d_v < 2$ µm and with increasing aggregate size could be distributed as small grains throughout the aggregate volume. The number abundance of this class was usually below 2 % in the collected samples.

2.2 Quartz-like and complex quartz-like

The classification of particles into quartz-like is relatively straightforward with a dominant Si signal. Some of the particles with high Si were also found with slightly higher Al content associated with them and are therefore classified as complex quartz-like. Fe content of quartz-like particles is generally low and variable, suggesting that Fe oxides are not an integral part of the quartz-like particles. The particle number abundance of quartz-like particles was ~ 8 % and complex quartz-like particles ranged from 1 % to 15 % depending on particle size.

2.3 Feldspar-like and pure feldspar abundance

The feldspar group is characterized by Si:Al:K / Si:Al:Na signal ratios of approximately 3:1:1 for microcline-like (K-feldspar) and albite-like (Na-feldspar), respectively. Ca-feldspar-like particles are quite rare in the samples. Na-feldspar particles are present across all size ranges ranging from 1.5 % in particles with $d_v < 2.5$ µm to around 3 % in particles with $d_v > 2.5$ µm. K-feldspar particles on the contrary are present in <1 % and are found mainly in particles with $d_v < 5$ µm. The complex feldspar-like and complex clay/feldspar mixture have Si:Al signal ratios of approximately 3:1 with additional elements such as Ca, Fe and Mg, suggesting a more complex aggregate than a pure feldspar. Complex feldspar-like particles were found in the range of 5 - 8 % in particles with $d_v < 20$ µm. For particles with $d_v > 20$ µm , its occurrence was about 15 %. Similar number abundances were also observed for complex clay/feldspar mixtures.

Regarding the identification of feldspars, there are two approaches: One is based on the classical ‘classification’ scheme, where a fixed limit around the usual composition of feldspars is used (detailed formalism in S1), and the other is the feldspar-

specific index approach, where a distance from the ideal composition is calculated. Both form different shapes in the x-dimensional element space and therefore lead to different results. The index approach has the advantage that it shows how close a particle is to an ideal composition. In this case, the feldspar indices regard the overall contribution of feldspar-specific elements to the particle and the specific Al/Si as well as alkali/Si or K/Si ratios. It was found that an index value of > 0.80 is suitable to distinguish between pure feldspar grains and other silicates. Details of the index calculation are given in S5.

2.4 Ca-rich

Calcium-rich particles include calcite-like, apatite-like, dolomite-like, and gypsum-like and these are characterized by high Ca, Ca+P, Ca+Mg, and Ca+S content, respectively. In gypsum-like the Ca:S weight ratio is ~ 1 and in dolomite-like particles the Ca:Mg weight ratio is ~ 1. Apatite-like particles were quite rare and only present in a few samples. The majority of the particles were calcite-like and their abundance was usually around 10 % for $d_v < 2.5$ µm and around 5 % for $2.5 < d_v < 10$ µm. This group did not include particles with appreciable Fe contents in contrast to other classes (Table. S3).

2.5 Clay minerals

Clay minerals can be divided into four subgroups: kaolinite-like, illite-like, smectite-like, and chlorite-like, with illite and kaolinite having a similar average Si-to-Al signal ratio (1.6 and 1.5 respectively), but with illite-like containing K, Fe and Mg whereas in kaolinite-like particles K is present in trace amount. These are the most abundant particle types found in the collected sample with number abundances of 25 % and 15 %, respectively. Smectite-like particles are clay minerals containing Fe and Mg, as well as small amounts of Ca and are found across all size ranges in small proportions (< 1 %). Chlorite-like particles are characterized by slightly higher Fe content compared to other clay minerals and their relative contribution is around 6 % in particles with $d_v < 2.5$ µm and 5 % in particles with $2.5 < d_v < 62.5$ µm.

2.6 Other silicates

The other silicate class group are characterized by the presence of Si and Al together with trace amounts of Mg, Ca, and Fe. Another silicate group in this class are Ca-rich silicates/Ca-Si-mixtures. These are typically clay minerals particles that are internally mixed with Ca carbonates (e.g. calcite). Furthermore, Fe is also a minor component in this particle class suggesting an additional contribution of Fe oxides. The particle number abundance of other silicates class is ~ 5 % and that of Ca-Si mixtures varies between 5 % to 12 % depending on particle size.

2.7 Sulfates

In the sulfate group, mainly ammonium sulfate-like particles were present (i.e. only S was detected in a particle). They make up a very small amount in the total sample (< 0.25 %) as individual particles and are mostly observed in particles with $d_v < 2$ µm. Ammonium sulfate is the prevalent sulfate species in atmospheric aerosols and generally of anthropogenic origin.

2.8 Mixtures and other

The silicate mixture group are dominated by Si along with the presence of other elements in varying amount and therefore does not belong to any other defined silicate group. The so-called 'other' group contains all particles that are not classified by the applied scheme into any of the groups described above. Therefore, it represents a mixture of different minerals or rare species. The relative number abundance for mixtures was around 4 % in the collected sample and the number percentage of the 'other' group is substantially low (< 0.5 %).

2.9 Silicate composition

The dominating composition in mineral dust is silicates which are composed of different minerals. Figure S1 shows the highly variable chemical composition of the silicate particles with (Mg+Fe)/Si ratio (x-axis), Al/Si ratio (y-axis), and the (Na+K+Ca)/Si ratio (z-axis, colour-coded) for each single particle. The three main clusters visible in Fig. S1 are numbered 1 (quartz-like), 2 (feldspar), and 3 (most other particles). Like mentioned in Kandler et al. (2011), the Al/Si ratio exhibits the least measurement uncertainty and varies significantly for different minerals. The (Mg+Fe)/Si ratio is an indicator for clay mineral aggregates as feldspar does not usually contain these elements (Anthony et al. (2003)). The (Na+K+Ca)/Si ratio can be used to differentiate between feldspar and clay minerals as feldspar shows much higher values as compared to clay minerals. However, it can be also seen that this distinction is usually not clear-cut as all dust particles are usually 'contaminated' with other minerals and the aggregates have ambiguous compositions.

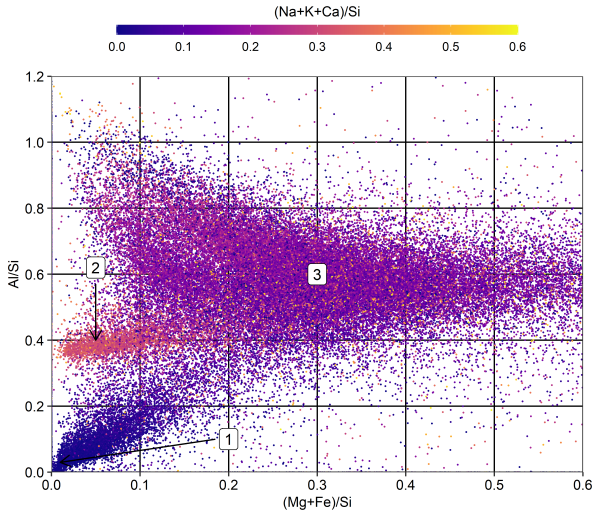

Figure S1. Scatter-plot for silicate particle composition. The three main clusters are marked by numbers: (1) quartz cluster, (2) feldspar cluster, and (3) clay mineral/aggregate cluster.

3 Size resolved elemental mass fraction

Table S2 presents the elemental mass fraction as a function of particle size and is calculated by dividing the average estimated elemental mass in a particle by the average estimated mass of particle.

Table S2. Elemental mass fraction as a function of particle size.

	Size class in μm						
Element	0.1-1	1-2	2-4	4-8	8-16	16-32	32-64
Na	0.006	0.004	0.004	0.006	0.005	0.006	0.008
Mg	0.025	0.027	0.029	0.029	0.029	0.03	0.027
Al	0.093	0.104	0.108	0.096	0.099	0.101	0.094
Si	0.199	0.217	0.226	0.231	0.243	0.25	0.265
P	0.002	0.001	0.001	0.001	0	0	0
S	0.012	0.005	0.003	0.002	0.002	0.002	0.002
Cl	0.002	0.002	0.002	0.004	0.002	0.003	0.003
K	0.023	0.027	0.029	0.027	0.027	0.029	0.031
Ca	0.059	0.05	0.047	0.059	0.049	0.04	0.032
Ti	0.009	0.004	0.003	0.004	0.003	0.002	0.002
Fe	0.078	0.072	0.061	0.049	0.047	0.047	0.046

Table S3. Average elemental composition (%) as a function of particle size for different particle groups. Elements with less than 3 % contribution is not mentioned.

	Size class in µm						
Particle type	0.1-1	1-2	2-4	4-8	8-16	16-32	32-64
Hematite-like	Fe.77 Si.11 Al.6	Fe.72 Si.14 Al.8	Fe.69 Si.16 Al.9	Fe.68 Si.16 Al.9	Fe.69 Si.16 Al.9		
Anatase-like	Ti.85 Si.7 Al.4	Ti.82 Si.9 Al.5	Ti.80 Si.9 Al.5	Ti.79 Si.11 Al.6			
Quartz-like	Si.92 Al.5	Si.91 Al.5	Si.90 Al.5	Si.89 Al.6	Si.88 Al.7	Si.88 Al.6	Si.87 Al.6
Complex quartz-like	Si.71 Al.13 Fe.5 Mg.5	Si.72 Al.13 Fe.5 Mg.5	Si.73 Al.13 Fe.4 Mg.4	Si.73 Al.13 Fe.4 Mg.4	Si.74 Al.13 Fe.4 Mg.4	Si.73 Al.13 Fe.4 Mg.5	Si.72 Al.13 Fe.4 Mg.5
Pyroxene-like	Si.52 Mg.38 Fe.5	Si.53 Mg.38 Fe.5	Si.53 Mg.42	Si.53 Mg.39	Si.53 Mg.38		
Albite-like	Si.56 Al.22 Na.18	Si.56 Al.22 Na.17	Si.56 Al.22 Na.16	Si.56 Al.22 Na.14	Si.56 Al.22 Na.14	Si.55 Al.22 Na.14	Si.56 Al.22 Na.13
Microcline-like	Si.55 Al.21 K.15	Si.57 Al.22 K.15	Si.57 Al.22 K.14	Si.57 Al.22 K.14	Si.57 Al.22 K.13	Si.57 Al.22 K.13	
Complex feldspar-like	Si.53 Al.22 K.10 Mg.4	Si.53 Al.22 K.9 Mg.5	Si.53 Al.22 K.8 Mg.6	Si.53 Al.22 K.6 Mg.6	Si.53 Al.22 K.6 Mg.6	Si.53 Al.22 K.5 Mg.7	Si.53 Al.22 K.6 Mg.7
Illite-like	Si.48 Al.30 K.8 Mg.6 Fe.6	Si.48 Al.30 K.7 Mg.7 Fe.7	Si.48 Al.30 K.7 Mg.6 Fe.6	Si.48 Al.30 K.7 Mg.6 Fe.5	Si.49 Al.30 K.7 Mg.6 Fe.5	Si.48 Al.29 K.7 Mg.6 Fe.5	Si.48 Al.28 K.7 Mg.6 Fe.5
Chlorite-like	Si.39 Al.25 Fe.21 Mg.9	Si.39 Al.25 Fe.20 Mg.10	Si.38 Al.25 Fe.20 Mg.11	Si.37 Al.25 Fe.22 Mg.10	Si.38 Al.26 Fe.20 Mg.11	Si.38 Al.25 Fe.19 Mg.13	Si.40 Al.26 Fe.16 Mg.10
Smectite-like	Si.41 Al.25 Mg.25 Fe.6	Si.40 Al.24 Mg.23 Fe.8	Si.40 Al.25 Mg.22 Fe.9	Si.40 Al.25 Mg.22 Fe.8	Si.40 Al.25 Mg.22 Fe.9	Si.40 Al.25 Mg.22 Fe.8	
Kaolinite-like	Si.50 Al.34 Fe.7 Mg.4	Si.50 Al.33 Fe.8 Mg.5	Si.50 Al.33 Fe.7 Mg.5	Si.50 Al.32 Fe.6 Mg.5	Si.51 Al.32 Fe.6 Mg.5	Si.50 Al.30 Fe.6 Mg.6	Si.50 Al.28 Fe.5 Mg.7
Palygorskite-like	Si.53 Mg.26 Al.17	Si.53 Mg.26 Al.15	Si.53 Mg.25 Al.15	Si.53 Mg.23 Al.16	Si.53 Mg.22 Al.16	Si.53 Mg.22 Al.17	
Ca-rich silicate/Ca-Si-mixture	Ca.47 Si.27 Al.13 Mg.5	Ca.47 Si.27 Al.13 Mg.5	Ca.46 Si.27 Al.14 Mg.6	Ca.44 Si.29 Al.14 Mg.6	Ca.42 Si.29 Al.14 Mg.6	Ca.39 Si.31 Al.15 Mg.7	Ca.37 Si.32 Al.16 Mg.7
Calcite-like	Ca.87 Si.6	Ca.83 Si.8	Ca.82 Si.9	Ca.82 Si.9	Ca.81 Si.10	Ca.82 Si.9	
Dolomite-like	Ca.49 Mg.43 Si.5	Ca.48 Mg.43 Si.5	Ca.46 Mg.44 Si.6	Ca.47 Mg.44 Si.6	Ca.48 Mg.42 Si.6	Ca.47 Mg.42 Si.6	
Apatite-like	Ca.55 P.37	Ca.52 P.41	Ca.50 P.47	Ca.51 P.38	Ca.54 P.31		
Gypsum-like	Ca.45 S.43 Si.5	Ca.45 S.44 Si.5	Ca.45 S.45 Si.5	Ca.44 S.46 Si.5	Ca.44 S.45 Si.6		
Ammonium-sulfate-like	S.94	S.94	S.98				
Complex sulfate	S.40 Na.24 Mg.21 Ca.11	S.38 Na.29 Mg.17 Ca.12	S.37 Na.28 Mg.8 Ca.15				
Halite-like	Na.46 Cl.40	Na.47 Cl.39	Na.46 Cl.41	Na.46 Cl.43	Na.47 Cl.44		

Table S4: Number fraction (%) of particles in each particle group per the dust size classification in Adebiyi et al. (2023) with 95 % confidence interval (CI).

Dust Size	Group	Relative Abundance	lower CI	upper CI
$D < 2.5$ μm	Albite-like	1.49	1.4	1.5
$2.5 < D < 10$ μm	Albite-like	1.97	1.9	2.1
$10 < D < 62.5$ μm	Albite-like	2.7	2.5	2.9
$D > 62.5$ μm	Albite-like	1.52	0.2	5.4
$D < 2.5$ μm	Ammonium-sulfate-like	0.36	0.3	0.4
$2.5 < D < 10$ μm	Ammonium-sulfate-like	0.05	0	0.1
$D < 2.5$ μm	Anatase-like	0.51	0.5	0.5
$2.5 < D < 10$ μm	Anatase-like	0.06	0	0.1
$10 < D < 62.5$ μm	Anatase-like	0.03	0	0.1
$D < 2.5$ μm	Apatite-like	0.33	0.3	0.4
$2.5 < D < 10$ μm	Apatite-like	0.45	0.4	0.5
$10 < D < 62.5$ μm	Apatite-like	0.06	0	0.1
$D < 2.5$ μm	Ca-rich silicate/Ca-Si-mixture	5.72	5.6	5.8
$2.5 < D < 10$ μm	Ca-rich silicate/Ca-Si-mixture	9.71	9.5	9.9
$10 < D < 62.5$ μm	Ca-rich silicate/Ca-Si-mixture	8.6	8.2	9
$D > 62.5$ μm	Ca-rich silicate/Ca-Si-mixture	5.3	2.2	10.6
$D < 2.5$ μm	Calcite-like	6.75	6.7	6.9
$2.5 < D < 10$ μm	Calcite-like	3.09	3	3.2
$10 < D < 62.5$ μm	Calcite-like	1.16	1	1.3
$D < 2.5$ μm	Chlorite-like	6.33	6.2	6.4
$2.5 < D < 10$ μm	Chlorite-like	3.23	3.1	3.4
$10 < D < 62.5$ μm	Chlorite-like	2.02	1.8	2.2
$D > 62.5$ μm	Chlorite-like	3.03	0.8	7.6
$D < 2.5$ μm	Complex clay-mineral-like	1.69	1.6	1.7
$2.5 < D < 10$ μm	Complex clay-mineral-like	2.14	2	2.2
$10 < D < 62.5$ μm	Complex clay-mineral-like	1.95	1.8	2.1
$D > 62.5$ μm	Complex clay-mineral-like	1.52	0.2	5.4
$D < 2.5$ μm	Complex clay/feldspar mixture	7.06	7	7.2
$2.5 < D < 10$ μm	Complex clay/feldspar mixture	7.55	7.4	7.7
$10 < D < 62.5$ μm	Complex clay/feldspar mixture	9.54	9.1	9.9
$D > 62.5$ μm	Complex clay/feldspar mixture	22.73	15.9	30.8

D < 2.5 μm	Complex feldspar-like	5.09	5	5.2
2.5 < D < 10 μm	Complex feldspar-like	8.29	8.1	8.5
10 < D < 62.5 μm	Complex feldspar-like	13.2	12.8	13.7
D > 62.5 μm	Complex feldspar-like	13.64	8.3	20.7
D < 2.5 μm	Complex mixture	0.15	0.1	0.2
2.5 < D < 10 μm	Complex mixture	0.07	0.1	0.1
10 < D < 62.5 μm	Complex mixture	0.09	0.1	0.1
D < 2.5 μm	Complex quartz-like	1.81	1.8	1.9
2.5 < D < 10 μm	Complex quartz-like	4.25	4.1	4.4
10 < D < 62.5 μm	Complex quartz-like	7.99	7.6	8.4
D > 62.5 μm	Complex quartz-like	21.97	15.2	30
D < 2.5 μm	Complex soluble salt	0.07	0.1	0.1
D < 2.5 μm	Complex sulfate	1.36	1.3	1.4
D < 2.5 μm	Dolomite-like	0.64	0.6	0.7
2.5 < D < 10 μm	Dolomite-like	0.52	0.5	0.6
10 < D < 62.5 μm	Dolomite-like	0.45	0.4	0.5
D < 2.5 μm	Gypsum-like	1.49	1.4	1.5
2.5 < D < 10 μm	Gypsum-like	0.8	0.7	0.9
10 < D < 62.5 μm	Gypsum-like	0.35	0.3	0.4
D < 2.5 μm	Halite-like	0.19	0.2	0.2
2.5 < D < 10 μm	Halite-like	0.39	0.3	0.4
10 < D < 62.5 μm	Halite-like	0.24	0.2	0.3
D < 2.5 μm	Hematite-like	2.37	2.3	2.4
2.5 < D < 10 μm	Hematite-like	0.42	0.4	0.5
10 < D < 62.5 μm	Hematite-like	0.11	0.1	0.2
D < 2.5 μm	Illite-like	25.22	25	25.4
2.5 < D < 10 μm	Illite-like	26.22	25.9	26.5
10 < D < 62.5 μm	Illite-like	21.52	21	22.1
D > 62.5 μm	Illite-like	10.61	5.9	17.2
D < 2.5 μm	Ilmenite-like	0.09	0.1	0.1
2.5 < D < 10 μm	Ilmenite-like	0.06	0	0.1
D < 2.5 μm	Kaolinite-like	14.8	14.7	14.9
2.5 < D < 10 μm	Kaolinite-like	15.09	14.8	15.3
10 < D < 62.5 μm	Kaolinite-like	14.03	13.6	14.5
D > 62.5 μm	Kaolinite-like	6.06	2.7	11.6

D < 2.5 μm	Mica-like	0.13	0.1	0.1
2.5 < D < 10 μm	Mica-like	0.13	0.1	0.2
10 < D < 62.5 μm	Mica-like	0.11	0.1	0.2
D < 2.5 μm	Microcline-like	0.31	0.3	0.3
2.5 < D < 10 μm	Microcline-like	0.56	0.5	0.6
10 < D < 62.5 μm	Microcline-like	0.6	0.5	0.7
D > 62.5 μm	Microcline-like	0.76	0	4.1
D < 2.5 μm	other	1	1	1
2.5 < D < 10 μm	other	0.41	0.4	0.5
10 < D < 62.5 μm	other	0.26	0.2	0.3
D > 62.5 μm	other	2.27	0.5	6.5
D < 2.5 μm	Other silicate	5.15	5.1	5.2
2.5 < D < 10 μm	Other silicate	4.81	4.7	5
10 < D < 62.5 μm	Other silicate	5.02	4.7	5.3
D > 62.5 μm	Other silicate	0.76	0	4.1
D < 2.5 μm	Palygorskite-like	0.25	0.2	0.3
2.5 < D < 10 μm	Palygorskite-like	0.36	0.3	0.4
10 < D < 62.5 μm	Palygorskite-like	0.57	0.5	0.7
D < 2.5 μm	Pyroxene-like	0.46	0.4	0.5
2.5 < D < 10 μm	Pyroxene-like	0.33	0.3	0.4
10 < D < 62.5 μm	Pyroxene-like	0.06	0	0.1
D < 2.5 μm	Quartz-like	6.99	6.9	7.1
2.5 < D < 10 μm	Quartz-like	6.9	6.7	7.1
10 < D < 62.5 μm	Quartz-like	7.18	6.8	7.5
D > 62.5 μm	Quartz-like	6.82	3.2	12.5
D < 2.5 μm	Silicate mixture	0.3	0.3	0.3
2.5 < D < 10 μm	Silicate mixture	0.49	0.4	0.5
10 < D < 62.5 μm	Silicate mixture	0.87	0.7	1
D > 62.5 μm	Silicate mixture	2.27	0.5	6.5
D < 2.5 μm	Smectite-like	1.02	1	1.1
2.5 < D < 10 μm	Smectite-like	1.28	1.2	1.4
10 < D < 62.5 μm	Smectite-like	1.01	0.9	1.2
D < 2.5 μm	Sodium sulfate	0.2	0.2	0.2
2.5 < D < 10 μm	Sodium sulfate	0.01	0	0
D < 2.5 μm	Sodium sulfate/silicate mixture	0.08	0.1	0.1

$2.5 < D < 10$ μm	Sodium sulfate/silicate mixture	0.02	0	0
$10 < D < 62.5$ μm	Sodium sulfate/silicate mixture	0.02	0	0
$D < 2.5$ μm	Sulfate/silicate mixture	0.49	0.5	0.5
$2.5 < D < 10$ μm	Sulfate/silicate mixture	0.26	0.2	0.3
$10 < D < 62.5$ μm	Sulfate/silicate mixture	0.19	0.1	0.3
$D > 62.5$ μm	Sulfate/silicate mixture	0.76	0	4.1

4 Determining the size distributions from the freewing impactor measurements

For calculating the atmospheric size distribution from the FWI, the collection efficiency of the FWI has to be considered.

The collection efficiency E(P) is parameterized from the experimentally determined values for discs given by May and Clifford (1967) as a function of impaction parameter *P*:

$$P = \frac{S}{D}, \tag{1}$$

where *S* is the stopping distance and *D* is the characteristic dimension, here 25 mm.

While *P* equals to the Stokes number within the Stokes regime, in the current work the particle Reynolds numbers are considerably higher. In this regime, in analogy to Hinds (1999) the stopping distance (*S*) can be approximated with better than 3 % accuracy as

$$S = \frac{\rho_{amb} \cdot d_{amb}}{\rho_a \cdot \sqrt{\gamma}} \left[Re_p^{1/3} - \sqrt{6} \tan\text{inverse}\left(\frac{Re_p^{1/3}}{\sqrt{6}} \right) \right], \tag{2}$$

where ρ_{amb} is the ambient particle density, estimated from chemical composition, ρ_a is air density, and γ is aerodynamic shape factor. Results of the trigonometric function must be given in radian. The dry aerodynamic shape factor is assumed as constant similar to Ott and Peters (2008).

The particle Reynolds number is calculated as

$$Re_p = \frac{\rho_a \cdot v_i \cdot d_{amb}}{\eta \cdot \sqrt{\gamma}} \tag{3}$$

where v_i = $\sqrt{v_r^2 + v^2}$ is the impaction velocity

v_r = $2\pi l f_r$ is the speed of the collector in the plane of rotation

l is the collector arm length

f_r is the rotation frequency

v is the wind speed

η is air viscosity

The collection E(P) efficiency for P>0.125 is then parameterized and the according correction is

$$c_e = \frac{1}{E(P)} = exp\left(\frac{0.28}{P} \right) \tag{4}$$

The total investigated volume (V_i) for the concentration calculations is determined by

V_i = Av_it_i, where

A is the analyzed area,

t_i is the sample collection time.

5 Calculation of the feldspar indices

The index values show the closeness of a particle composition to pure feldspar. They are composed of three properties, the overall contribution of feldspar-specific elements to the particle composition and the closeness to the feldspar Al/Si ratio as well as to the K/Si or alkali/Si ratio. The overall contribution of specific elements is calculated as

$$r_{Sil} = \frac{|Na| + |Al| + |Si| + |K| + |Ca|}{|Na| + |Al| + |Si| + |K| + |Ca| + |Mg| + |P| + |S| + |Cl| + |Ti| + |Fe|} \tag{5}$$

Closeness w.r.t Al/Si is determined as

$$r_{fsp,Al/Si} = \frac{|Al|}{|Si|} \frac{3|Na| + 3|K| + 2|Ca|}{|Na| + |K| + 2|Ca|} \tag{6}$$

$$Q_{fsp,Al/Si} = \begin{cases} 1 - \left| lg(r_{fsp,Al/Si}) \right| & \forall \quad 0.1 \leq r_{fsp,Al/Si} \leq 10 \\ 0 & \forall \quad r_{fsp,Al/Si} < 0.1 \\ 0 & \forall \quad r_{fsp,Al/Si} > 10 \end{cases} \tag{7}$$

Closeness w.r.t K and alkali ratio is calculated as

$$r_{fsp,K/Si} = \frac{3|K|}{|Si|} \tag{8}$$

$$Q_{fsp,Al/Si} = \begin{cases} 1 - \left| lg(r_{fsp,K/Si}) \right| & \forall \quad 0.1 \leq r_{fsp,K/Si} \leq 10 \\ 0 & \forall \quad r_{fsp,K/Si} < 0.1 \\ 0 & \forall \quad r_{fsp,K/Si} > 10 \end{cases} \tag{9}$$

$$r_{fsp,NaKCa/Si} = \frac{3|Na| + 3|K| + 2|Ca|}{|Si|} \tag{10}$$

$$Q_{fsp,Al/Si} = \begin{cases} 1 - \left| lg(r_{fsp,NaKCa/Si}) \right| & \forall \quad 0.1 \leq r_{fsp,NaKCa/Si} \leq 10 \\ 0 & \forall \quad r_{fsp,NaKCa/Si} < 0.1 \\ 0 & \forall \quad r_{fsp,NaKCa/Si} > 10 \end{cases} \tag{11}$$

The similarity of a particle's composition to pure feldspar in expressed then as

$$P_{fsp} = r_{Sil} Q_{fsp,Al/Si} Q_{fsp,NaKCa/Si} \tag{12}$$

and to pure K-feldspar as

$$P_{fsp,K} = r_{Sil} Q_{fsp,Al/Si} Q_{fsp,K/Si} \tag{13}$$

For example, the P_{fsp} value becomes 1 for pure microcline or plagioclase and 0 for sodium chloride or quartz.

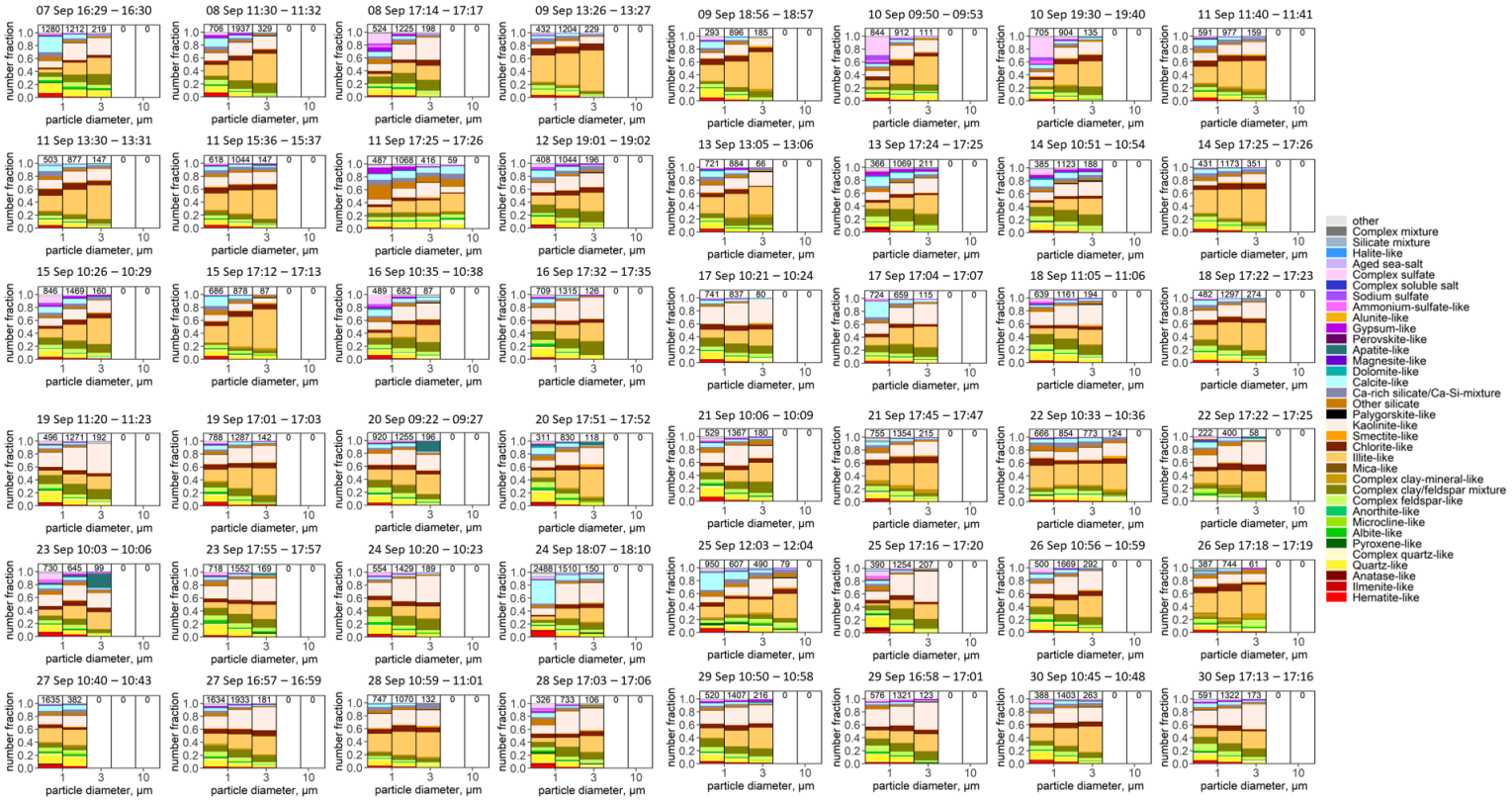

Figure S2. Number abundance for MOUDI stage 4. Abundance bars are not shown for size bins with fewer than 50 particles.

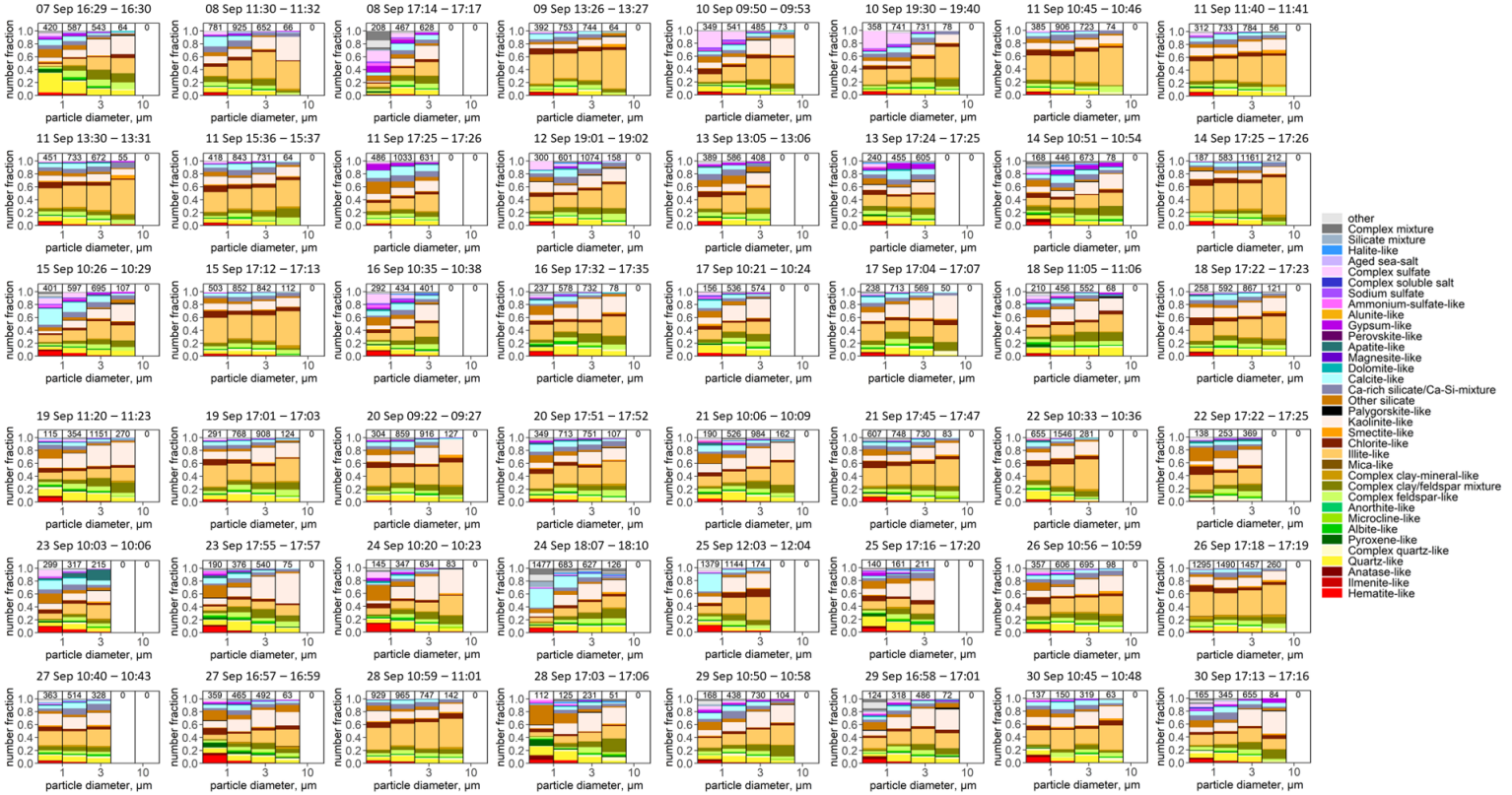

Figure S3. Number abundance for MOUDI stage 3. Abundance bars are not shown for size bins with fewer than 50 particles.

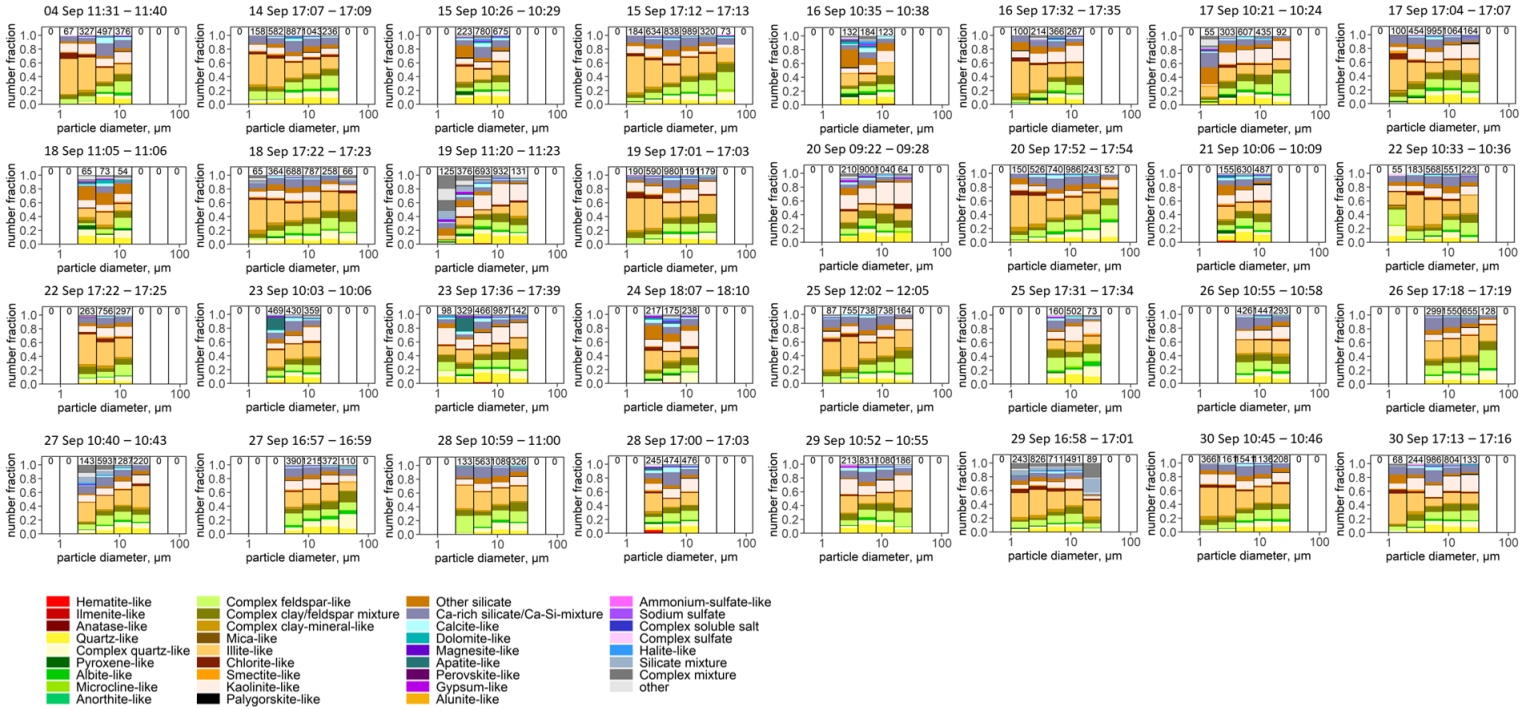

Figure S4. Number abundance for FWI. Abundance bars are not shown for size bins with fewer than 50 particles.

References

Adebiyi, A., Kok, J. F., Murray, B. J., Ryder, C. L., Stuut, J.-B. W., Kahn, R. A., Knippertz, P., Formenti, P., Mahowald, N. M., Pérez García-Pando, C., Klose, M., Ansmann, A., Samset, B. H., Ito, A., Balkanski, Y., Di Biagio, C., Romanias, M. N., Huang, Y., and Meng, J.: A review of coarse mineral dust in the Earth system, Aeolian Research, 60, 100 849, https://doi.org/10.1016/j.aeolia.2022.100849, 2023.

Anthony, J. W., Bideaux, R. A., Bladh, K., and Nichols, M. C.: Handbook of Mineralogy, Mineralogical Society of America, Chantilly, VA 20151-1110, USA, 2003.

Hinds, W. C.: Aerosol technology: properties, behavior, and measurement of airborne particles, John Wiley & Sons, 1999.

Kandler, K., Lieke, K., Benker, N., Emmel, C., Küpper, M., Müller-Ebert, D., Ebert, M., Scheuvens, D., Schladitz, A., Schütz, L., and Weinbruch, S.: Electron microscopy of particles collected at Praia, Cape Verde, during the Saharan Mineral Dust Experiment: particle chemistry, shape, mixing state and complex refractive index, Tellus B: Chemical and Physical Meteorology, 63, 475–496, https://doi.org/10.1111/j.1600-0889.2011.00550.x, 2011.

May, K. R. and Clifford, R.: The Impaction of Aerosol Particles on Cylinders, Spheres, Ribbons and Discs, The Annals of Occupational Hygiene, 10, 83–95, https://doi.org/10.1093/annhyg/10.2.83, 1967.

Ott, D. K. and Peters, T. M.: A Shelter to Protect a Passive Sampler for Coarse Particulate Matter, PM10 - 2.5, Aerosol Science and Technology, 42, 299–309, https://doi.org/10.1080/02786820802054236, 2008.